Russian Geology and Geophysics © 2019, V.S. Sobolev IGM, Siberian Branch of the RAS
Vol. 60, No. 4, pp. 386–399, 2019 *DOI:10.15372/RGG2019088* *Geologiya i Geofizika*

High-Grade Contact Metamorphism in the Kochumdek River Valley (Podkamennaya Tunguska Basin, East Siberia): Evidence for Magma Flow

E.V. Sokol [a], O.P. Polyansky [a, ✉], A.N. Semenov [a], V.V. Reverdatto [a], S.N. Kokh [a], A.S. Devyatiyarova [a], V.Yu. Kolobov [a], P.V. Khvorov [b], A.V. Babichev [a]

[a] *V.S. Sobolev Institute of Geology and Mineralogy, Siberian Branch of the Russian Academy of Sciences, pr. Akademika Koptuga 3, Novosibirsk, 630090, Russia*

[b] *Institute of Mineralogy, Ural Branch of the Russian Academy of Sciences, Miass, 456317, Russia*

Received 9 April 2018; received in revised form 14 June 2018; accepted 17 September 2018

Abstract—Spurrite-merwinite marbles on the right bank of the Kochumdek River in the Podkamennaya Tunguska basin formed along the top margin of a flood basalt intrusion (Kuzmovka complex) from a marly limestone protolith of the Rhuddanian Lower Kochumdek Subformation, at a pressure of ~200 bars. The contact metamorphic aureole comprises four zones of successively decreasing temperatures marked by the respective mineral assemblages: $T \geq 900$ °C (merwinite, spurrite and gehlenite (±rankinite, bredigite); $T \geq 750$ °C (spurrite); $T \geq 700$ °C (tilleyite, wollastonite, and melilite ($Gehl_{<50}$)); and ~500–550 °C (diopside, amphibole, and grossular). Very high temperatures at the contact ($T_{cont} > 2/3\ T_{melt}$) result from magma flow along a conduit. The temperature profiles for the Kochumdek metamorphic complex show good fit between measured and geothermometer-derived values at a magma temperature of 1200 °C, an intrusion thickness of ≥ 40 m, a heating time of six months, and a magma flow lifespan within one month. Stagnant magma in a conduit of any thickness cools down and crystallizes rapidly and fails to heat up sediments to the temperatures required for spurrite–merwinite metamorphism (above 790 °C).

Keywords: contact metamorphism, spurrite–merwinite facies, Kuzmovka complex traps, simulation, indicator minerals, East Siberia

INTRODUCTION

Rocks produced by high-temperature contact metamorphism arouse stable interest because their origin remains poorly understood in many aspects: *PT*-conditions, heat transfer between igneous bodies and country rocks, duration of prograde and retrograde metamorphic events, isotope exchange, and mobility of major and trace elements (Reverdatto, 1970; Pertsev, 1977; Kerrick, 1991; Heinrich et al., 2004; Grapes, 2011). Spurrite-merwinite facies rocks ($T > 800$°C) are commonly related with mafic intrusions and either occur along magma conduits (dikes, vents, necks, etc.) or are enclosed as xenoliths in gabbro, alkali basalts, ignimbrites, etc. (Reverdatto, 1970; Koritnig, 1978; van Bergen and Barton, 1984; Kerrick, 1991; Galuskina et al., 2010; Grapes, 2011; Galuskin et al., 2012; Gazeev et al., 2012). These metamorphic rocks most often form one or more narrow zones adjacent to intrusions and contain uniform mineral assemblages of few phases. Meanwhile, boundary conditions in thermophysical problems should be formulated with reference to data from zoned complexes where each mineral assemblage is actually a temperature marker. This study focuses on the metamorphic zonation and temperature distribution in spurrite-merwinite marbles from the Kochumdek River valley, Podkamennaya Tinguska basin, Siberian craton (Fig. 1), and the heat source of metamorphism; the heat transfer problem is solved by modeling.

✉ Corresponding author.
E-mail adress: pol@igm.nsc.ru (O.P. Polyansky)

HISTORIC BACKGROUND

Contact metamorphic rocks in the Kochumdek River basin were discovered more than sixty years ago (Malich and Grigoriev, 1960). In 1960, Reverdatto (1964) found spurrite produced by isochemical metamorphism in the area. Later on, sampling of scattered marble blocks and a fragment of the marble-dolerite contact in 1970 and 1973 led to discovery of merwinite and spurrite-monticellite symplectites (Pertsev and Shmulovich, 1972; Pertsev, 1977). The field trip by Kolobov (1981) was the most successful, as the contact between the intrusion and the overlying marly limestone was exposed in a bluff and spurrite-merwinite marbles were open for sampling. In 2017 we sampled other marble zones and the protolith sediments of the lower Kochumdek subformation ($S_1k\check{c}_1$).

GEOLOGICAL BACKGROUND

The local geology of the Podkamennaya Tunguska right bank in the middle reaches of the river includes Paleozoic

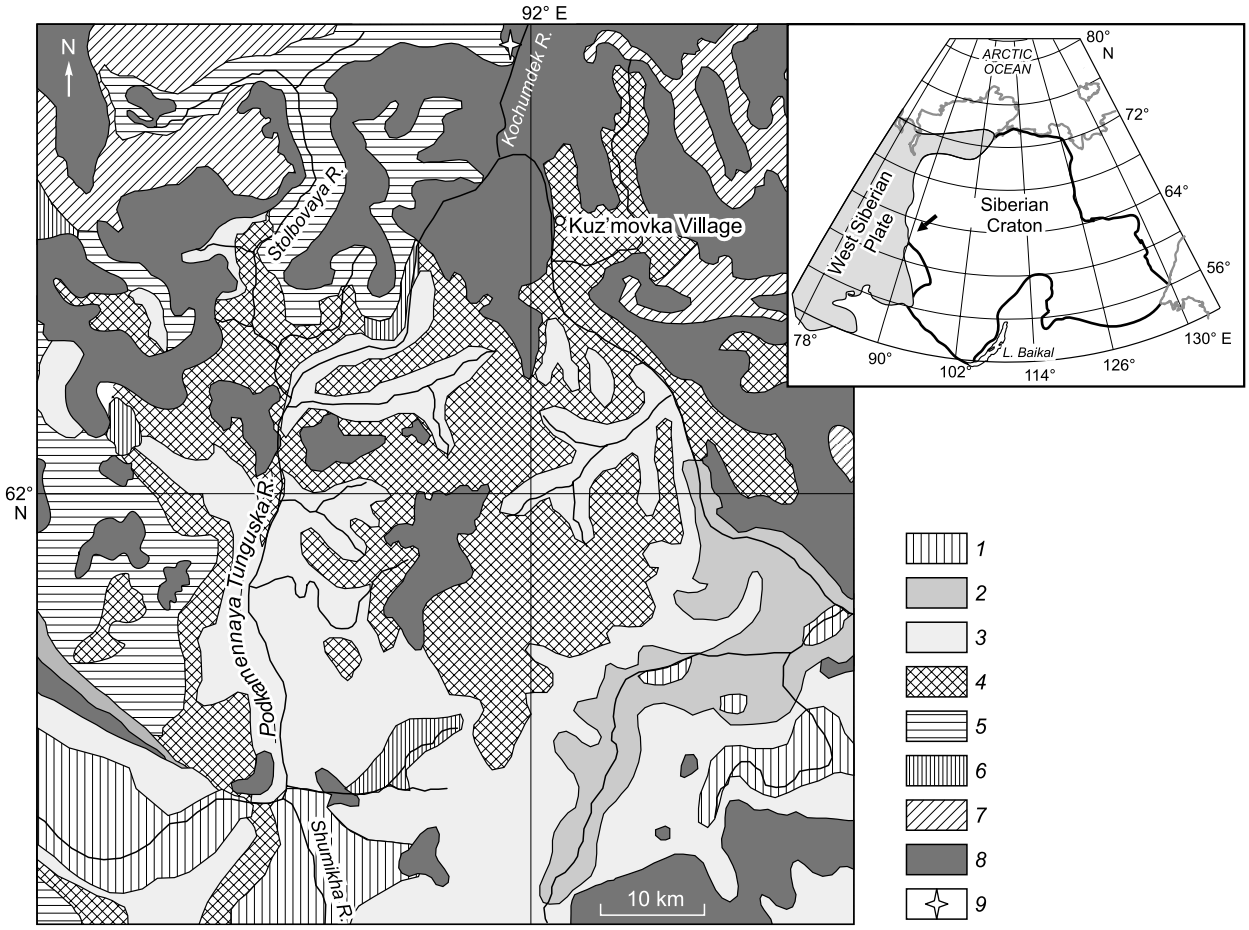

Fig. 1. Simplified geology of the study area, after (Lebedev, 1962). *1*, Upper Evenki subformation (Upper Cambrian); *2*, Lower Ordovician Baikit, Chunya and Proletarskaya (undifferentiated) formations; *3*, Middle Ordovician Krivye Luki and Mangaseya stages (undifferentiated); *4*, Upper Ordovician Dolbor stage; *5*, Lower Silurian (Llandovery); *6*, Middle Devonian Yukta and Tynep formations (undifferentiated); *7*, Upper Permian; *8*, Early Triassic intrusions of Kuzmovka complex; *9*, Kochumdek contact metamorphic complex. Legend corresponds to State Geological Map (1976), scale 1: 200 000. Ser. Turukhansk, Sheet R-46-XIV (Poryadin et al., 1977).

sediments (O–P), Tertiary continental flood basalts (traps) of the Kuzmovka complex ($\nu\beta T_1kz$), and Quaternary ($Q_{II–III}$) glacial deposits (Lungershausen, 1959; Poryadin et al., 1977; Alekseenko et al., 2010). The sedimentary sequences dip monoclinally at low angles (a few degrees) to the northeast, inward the Tunguska basin. The subsided northeastern part of the area is heavily faulted. Llandovery sediments (S_1ln), up to 140 m thick, occupy the largest surface area within map sheet R-46-IV. A complete section of younger Paleozoic sediments ($S_1w–P_2pl$) remained preserved only in subsided blocks (Poryadin et al., 1977; Alekseenko et al., 2010) (Fig. 1). The total thickness of Paleozoic sediments that lied over the Llandovery limestone at the time of the Kuzmovka intrusion reached 525 m. The 140 m S_1ln sequence contributed to the total overburden pressure during contact metamorphism sicne intrusions within the Kochumdek block occurred also at the Silurian–Ordovician boundary.

The Kochumdek Formation is composed of siltstone and limestone in the 56–66 m carbonate-clastic upper unit ($S_1kč_2$) and limestone with thin siltstone or mudstone intercalations and disseminated sulfides in its 62–64 m lower unit (Rhuddanian, $S_1kč_1$). The lowermost section includes two marker beds of (i) dolomitic limestone with sulfides and bituminous shale layers and (ii) marly limestone with rhythmically alternated wavy layers consisting of abundant kaolinite and lesser percentages of hydromica (Tesakov, 2014; Alekseenko et al., 2010).

Trap intrusions make up several $PZ_3–MZ_1$ tholeiite-dolerite complexes in the right side of the Podkamennaya Tunguska: Tymer, Katanga (βT_1kt, undifferentiated gabbro-dolerite), Kuzmovka ($\nu\beta T_1kz$, differentiated gabbro-dolerite), and Surinda (β-νT_1sr, weakly differentiated gabbro-dolerite). Igneous rocks reach the greatest thicknesses and surface areas in large basins (e.g., up to 530 m thick in the Bakhta basin) and at intersections of regional-scale faults, but they are only 120–250 m thick among PZ_1 sediments in the Delig-Kochumdek uplift. They occupy up to 50% of the $PZ_{2–3}$ section and 25% in the PZ_1 part (Lebedev, 1962;

Prusskaya, 2008; Alekseenko et al., 2010; Egorova and Latypov, 2013). Within the sampled area, the Kuzmovka rocks occur as low-angle multistage sills, dikes, and veins (Alekseenko et al., 2010; Lungershauzen et al., 1959; Poryadin et al., 1977). Sills, which intrude mainly Ordovician and Silurian sediments, are subalkaline differentiates. Dikes are commonly nearly vertical or dipping at high angles, from a few meters to 260 m thick and from 500 m to 5 km long. The bodies grade smoothly from one to another and thus must belong to a single complex. The Kuzmovka dolerites are mainly troctolitic while olivine dolerites and gabbro-dolerites occur most often near the base and in the middle of intrusions and trachytic varieties coexist with ferrogabbro in the middle and uppermost parts. Most strongly differentiated large sills contain granophyres and quartz or pegmatictic dolerites (Poryadin et al., 1977; Egorova and Latypov, 2013). In the Kochumdek valley, the differentiated Kuzmvosky intrusions form a series of olivine and troctolite dolerites to quartz gabbro-dolerite varieties (Lungershauzen et al., 1959; Reverdatto, 1964; Alekseenko et al., 2010).

Rocks within the Kuzmovka complex are locally metamorphosed and metasomatised: minor amounts of secondary hornfels and quartz are associated with small sills and dikes while skarns or less often pyroxene, pyroxene-garnet, amphibole and epidote hornfels, marbles, and calciphyres occur among differentiated intrusions (Reverdatto, 1964, 1970; Pertsev, 1977; Poryadin et al., 1977; Alekseenko et al., 2010); metamorphism in large sills has produced pyroxene and hornblende hornfels facies (Reverdatto, 1964). Shales are occasionally converted to buchites with glass and grains of bitownite, pigeonite, tridymite, mullite, and cordierite which are known to form at temperatures no lower than 870 °C (Reverdatto, 1970; Pertsev, 1977; Alekseenko et al., 2010).

A bluff exposure of the Kochumdek Formation marmorized marly limestone in the right side of the Podkamennaya Tunguska provides an example of high-temperature metamorphism at the contact with a 150 m thick sill (Reverdatto, 1964; Pertsev, 1977). The sill consists of olivine and olivine-hypersthene dolerite in its lower part, hypersthene dolerite in the middle, and dolerite-pegmatite segregations with iron-rich olivine among quartz-feldspar interstitial material near the top. The top margin of the sill is delineated by a 0.5–0.7 m thick quench zone and a 1–3 cm zone of garnet skarn.

High-temperature marbles near the upper sill margin reach a total thickness of 1.5 m, out of which 0.3–0.4 m of fine (<1 mm) spurrite marble. Coarse marble (0.7–1.2 m thick) contains sporadic grains of tilleyite and spurrite free from reaction rims, which coexist with later vesuvian, garnet, and hydrogrossular. Other zones of the aureole are: 1–2 m thick melilite-wollastonite marble, with melilite replaced by garnet or vesuvian; 5 m thick garnet-pyroxene marble with wollastonite (2.5–3.5 m above the contact); a partly recrystallized carbonate matrix and Ca silicates along shale layers (7–9 m above the contact). Metamorphism at the sill base is of lower grade, with hydrothermally altered marbles.

MATERIALS AND METHODS

Seventy samples collected from the Kochumdek area in 1981 and 2017 were analyzed at the Analytical Center for Multielement and Isotope Studies of the V.S. Sobolev Institute of Geology and Mineralogy (IGM, Novosibirsk). Petrography and mineralogy were examined using *Olympus BX 51* and *Zeiss Axio A1* light microscopes and a Tescan *Mira 3-LMU* scanning electron microscope. Mineral chemistry was analyzed by EMPA on a *Mira 3-LMU* scanning electron microscope with an Oxford Instruments *INCA Energy 450+ XMax80* analyzer, as well as on *Camebax-Micro* and Jeol *JXA–8100* microanalyzers. For details of the method see (Khoury et al., 2016; Sokol et al., 2016). Major-element chemistry of rocks was analyzed by XRF at IGM (Novosibirsk) and by wet chemistry at the Vinogradov Institute of Geochemistry (Irkutsk). X-ray powder diffraction analysis was performed on a *Shimadzu XRD-6000* diffractometer (Cu anode, graphite monochromator) at the Institute of Mineralogy (Miass). Crystalline phases were quantified in *Siroquant V4* by the Rietveld method.

CONTACT METAMORPHISM IN THE KOCHUMDEK RIVER VALLEY

Marmorized limestones and marbles crop out in the right side of the Kochumdek River (right tributary of the Podkamennaya Tunguska), 16–17 km upstream of the mouth, at 62°27′54.59″ N, 91°55′42.99″ E (Fig. 1). Llandovery (S_1ln) carbonate sediments became metamorphosed under the effect of an intrusion of the Kuzmovka complex (T_1) that lies below (Malich and Grigoryev, 1960; Pertsev and Shmulovich, 1972; Pertsev, 1977; Reverdatto, 1964, 1970). The intrusion located at an elevation of ~100 m within a 14 km segment upstream of the mouth obstructs the Kochumdek River incision. The steep valley sides expose Ordovician (120–200 m) and Llandovery (200–320 m) sediments and two sills at elevations of 410–360 m and 320–280 m, respectively. Alternated gabbro and limestones (S_1kč), including marbled limestones of the lower Kochumdek subformation, crop out within a 5 km long segment of the Kochumdek valley upstream of the Maiguchar River inlet.

The geometry of the intrusion responsible for metamorphism is hard to constrain because of poor exposure. It was interpreted as a 70–90 m thick dike dipping northward at a low angle, with high-temperature metamorphics in the northern part of the aureole along its hanging wall and lower-temperature rocks in the southern part along the footwall (Reverdatto, 1964; Pertsev, 1977). Or, the body may have an undulated top, with igneous rocks exposed in swells and marmorized marly limestone in sags (Fig. 2).

The lower Kochumdek marmorized marly limestones appear in the southern part of the complex as scattered blocks lying immediately over the intrusion near the water and in a low-elevated right-bank floodplain. Most of marble blocks

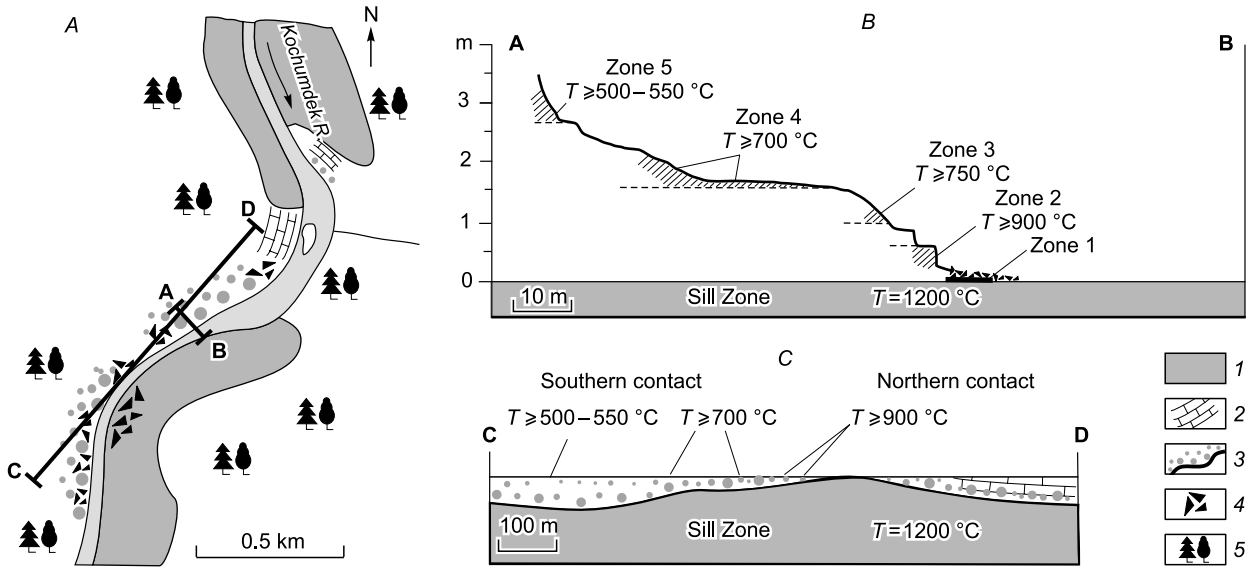

Fig. 2. Schematic map (*A*) and simplified cross sections of Kochumdek contact metamorphic complex (*B*, *C*). Left vertical axis shows thickness of metamorphic aureole (m). Zero level is at intrusion top. *1*, Kochumdek intrusion; *2*, marly limestone of lower Kochumdek subformation; *3*, marbles (large and small circles are high- and low-temperature rocks, respectively); *4*, scattered rock blocks; *5*, taiga. Cross sections along lines A–B and C–D. Dash lines correspond to sampling sites.

are autochthonous and retain nearly horizontal bedding. Upside down blocks are rare and restricted to near-water sites. Judging by angular shapes of the blocks, with sharp or weakly rounded edges, the marbles became exposed quite recently, during the current postglacial erosion. Those exposed at the floodplain level contain tremolite and/or wollastonite and grossular. Tilleyite marbles lie 2–3 m below, where the contact with the intrusion remains invisible. Spurrite-merwinite marbles were discovered in bedrock exposures in the northern part of the area in 1981, when the river had a low stand. They crop out along the bluff in a nearly horizontal strip, about 150 m long and 30 cm thick, lying

Table 1. Major oxides in gabbro from the Kochumdek intrusion top (wt.%)

Sample	1	2	3	4	5	6	7	8	9
	PT-95	PT-95-a	PT-96	PT-101	PK-4-8	PK-7-1	PT-114	PK-9-2	PK-9-1*
SiO_2	47.43	48.63	48.74	50.06	48.01	47.35	48.80	45.65	48.27
TiO_2	1.93	1.81	1.19	1.13	1.86	1.75	1.60	4.07	2.46
Al_2O_3	9.82	10.28	9.43	8.23	16.12	14.44	15.91	11.87	14.20
Fe_2O_3	14.46	13.53	11.14	11.86	13.79	14.80	13.33	21.25	16.91
MnO	0.27	0.26	0.22	0.22	0.20	0.23	0.20	0.28	0.25
MgO	6.03	5.86	8.90	9.97	4.97	6.30	5.04	3.93	4.21
CaO	15.44	15.06	14.83	16.27	10.06	10.20	11.38	8.54	9.60
Na_2O	2.00	2.06	2.19	1.49	3.02	2.72	2.80	2.86	2.92
K_2O	1.20	1.37	0.87	0.39	0.64	0.67	0.58	0.81	0.82
P_2O_5	0.24	0.26	0.10	0.10	0.25	0.19	0.19	0.39	0.28
SO_3	0.13	0.10	0.14	<0.03	0.14	<0.03	<0.03	0.07	<0.03
LOI	0.85	0.91	2.42	–0.13	0.12	0.63	0.10	–0.34	–0.12
Total	99.80	100.13	100.17	99.59	99.18	99.28	99.93	99.38	99.80
H_2O	0.80	0.90	0.90	0.70	–	–	–	–	–
T_{liq}, °C	1214	1206	1214	1227	1218	1200	1225	1238	1212

Note. BaO, V_2O_5, Cr_2O_3, NiO < 0.1 wt.%. H_2O is according to thermal analysis. Mineral assemblages (from XRD and optical microscopy): 1–3, Cpx–Pl–Bt (± Opx, Kfsp, Amp, Chl); 4–6, 9, Cpx–Pl–Bt (± Kfsp, Amp, Chl); 7–8, Cpx–Pl–Bt–Amph (± Ol, Kfsp, Chl). Amp, amphibole; Bt, biotite; Chl, ckhlorite; Cpx, clinopyroxene; Kfsp, K-feldspar; Ol, olivine; Opx, orthopyroxene; Pl, plagioclase. Liquidus temperatures are calculated in *MELTS* (Ghiorso et al., 1995).

* Dike and other Kochumdek igneous rocks.

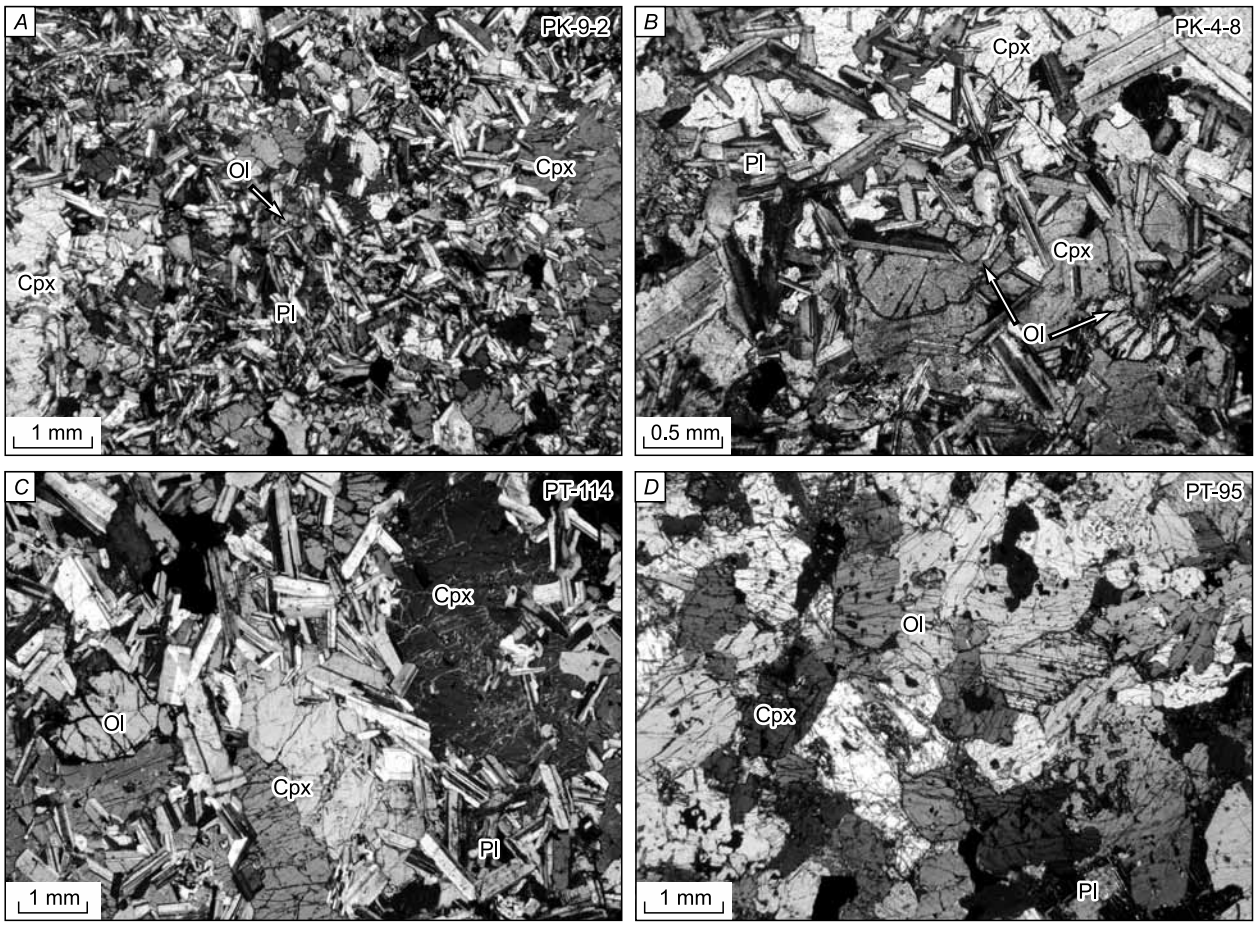

Fig. 3. Igneous rocks from contact metamorphic site in the Kochumdek River valley. Dikes (*A*) with coarse clinopyroxenes, plagioclase laths and interstitial olivine grains. Troctolite gabbro-dolerite from the top of Kochumdek intrusion (*B–D*) bearing coarse augite and olivine with interstitial plagioclase. Petrographic thin sections. Cross polarized light images. Cpx, clinipyroxene; Ol, olivine; Pl, plagioclase.

above a zone of debris (20—30 cm) which lies immediately over the intrusion. No metamorphic zonation related to the crosscutting dike is evident.

The intrusion top, sampled over ~1 km, is composed of medium (0.5–8 mm) gabbro, gabbro-dolerite, and olivine and troctolite dolerites (Fig. 3, Table 1). It lacks any quench zone but contains lenses of coarse grains up to 2 cm. The mineralogy consists of clinopyroxene, plagioclase, and olivine reaching, respectively, 56, 69, and 5%. Plagioclase is mostly fine, located in interstitials, while coarse laths are commonly grown together with olivine or clinopyroxene (Fig. 3). There are also small percentages of coarse flaky biotite (2–9%), brown and greenish-blue fine acicular amphibole (1–5%), and chlorite (1–4%) that replace pyroxene. Main accessory phases are ilmenite, titanomagnetite, titanite, apatite-(F,Cl), and pyrrhotite; secondary accessories include baddeleyite, zircon, pentlandite, sphalerite, and cobaltite. Zeolite-scapolite rocks with > 1 wt.% Cl occur within the northern contact.

The Kochumdek olivines contain 36.3–55.0 wt.% FeO and as low as ≤1.1 wt.% MnO and show weak zonation, with FeO 1–2 wt.% higher in rims than in cores (Table 2). Clinopyroxenes are unzoned augites with variable compositions ($En_{23–46}Fs_{14–39}Wol_{28–44}$); pigeonites ($En_{25–27}Fs_{62–67}Wol_{7–11}$) are rare, and orthopyroxenes ($En_{47}Fs_{49}Wol_3$) are extremely rare. Plagioclases have distinct zonation with compositionally different cores ($An_{55–82}Ab_{17–42}Ort_{0.5–2.5}$) and rims ($An_{51–63}Ab_{35–46}Ort_{1.6–2.7}$) in small laths, and still more contrasting coarse laths ($An_{46–68}Ab_{30–52}Ort_{1.5–2.7}$ and $An_{1–19}Ab_{79–96}Ort_{0.0–2.5}$ rims). Feldspar ($Ort_{85–100}Ab_{0–14}An_{0–1.5}$) forms antiperthites in plagioclase and rarely occurs as isolated grains coexisting with Cl-bearing apatite in interstitials. Biotite contains 29–39 wt.% FeO and within 4 wt.% TiO_2, 1.2 wt.% V_2O_3, and 4.5 wt.% Cl. Chlorine is also present in amphibole (0.4–1.6 wt.%), chlorite (0.1–0.5 wt.%), and apatite (0.5–2.8 wt.%); the latter also bears 1.3–3.8 wt.% F and ≤1 wt.% SrO.

The Kochumdek marbles are dense fresh rocks with a coarse banded structure produced by their original lithological heterogeneity (Fig. 4*a*, *b*): alternated light gray (mainly calcitic) and darker (silicate) 0.1–2.0 cm layers. Merwinite marbles have the coarsest grains of 0.5–4 mm to 1–2 cm (Pertsev, 1977). All metamorphic rocks were derived from a single carbonate and marl unit of the lower Kochumdek sub-

Table 2. Representative analyses of rock-forming minerals in gabbro from the Kochumdek intrusion top (wt.%)

Component	LLD	1	2	3*	4*	5	6	7	8	9*	10	11	12*	13*	14*
		Ol				Aug		Pgt		Opx	Pl				Kfsp
SiO_2	0.02	32.50	32.44	35.39	35.56	50.43	50.38	48.35	49.20	51.92	47.70	52.91	55.71	65.74	65.21
TiO_2	0.03	bd.	bd.	<0.30	<0.30	0.90	0.66	0.14	0.19	<0.30	bd.	0.06	<0.30	<0.30	<0.30
Al_2O_3	0.03	bd.	bd.	<0.30	<0.30	1.45	1.11	0.17	0.26	<0.30	32.29	28.54	27.72	21.56	18.31
FeO	0.06	51.54	52.78	36.89	36.33	14.71	16.14	38.58	35.14	30.19	0.60	0.75	0.35	<0.30	<0.30
MnO	0.06	0.93	0.89	0.56	0.55	0.33	0.44	0.85	0.86	0.65	bd.	bd.	<0.30	<0.30	<0.30
MgO	0.04	14.12	13.73	26.99	27.52	11.04	11.04	8.24	8.47	16.40	0.06	0.08	<0.30	<0.30	<0.30
CaO	0.02	bd.	bd.	0.16	0.15	20.21	19.14	4.09	4.75	1.47	16.54	12.59	9.95	2.48	<0.30
Na_2O	0.05	bd.	bd.	0.05	<0.30	0.36	0.39	0.06	0.19	<0.30	2.02	4.24	5.74	10.12	0.73
K_2O	0.02	bd.	bd.	<0.30	<0.30	bd.	bd.	bd.	bd.	<0.30	bd.	0.30	0.34	0.31	15.48
Total	–	99.09	99.84	100.04	100.10	99.44	99.30	100.49	99.05	100.63	99.21	99.46	99.81	100.21	99.73
Formula based on	–	4 O**				6 O**					8 O**				
Si	–	0.995	0.999	0.993	0.993	1.942	1.952	1.975	2.007	2.002	2.515	2.885	2.208	2.420	3.004
Ti	–	0.000	0.000	0.000	0.000	0.026	0.019	0.004	0.006	0.000	0.000	0.000	0.000	0.000	0.000
Al	–	0.000	0.000	0.000	0.000	0.066	0.051	0.008	0.012	0.000	1.475	1.115	1.762	1.539	0.994
Fe	–	1.353	1.324	0.865	0.848	0.473	0.522	1.317	1.198	0.973	0.013	0.000	0.023	0.000	0.000
Mn	–	0.023	0.024	0.013	0.013	0.011	0.014	0.029	0.030	0.021	0.000	0.000	0.000	0.000	0.000
Mg	–	0.627	0.646	1.127	1.144	0.633	0.637	0.501	0.514	0.941	0.000	0.000	0.000	0.000	0.000
Ca	–	0.000	0.000	0.005	0.004	0.834	0.794	0.179	0.208	0.061	0.481	0.117	0.820	0.617	0.000
Na	–	0.000	0.000	0.003	0.000	0.027	0.029	0.005	0.015	0.000	0.503	0.862	0.182	0.377	0.065
K	–	0.000	0.000	0.000	0.000	0.000	0.000	0.000	0.000	0.000	0.000	0.017	0.006	0.018	0.910

Note. P_2O_5 < 0.02 wt.%. LLD, detection limits of respective component; bd, below detection limit. Analyses 1, 3, 5, 7, 11, 12, 14 are for core; analyses 2, 4, 6, 8, 13, 15 are for rim. 1, $Fo_{31.67}Fa_{68.33}$; 2, $Fo_{32.80}Fa_{67.20}$; 3, $Fo_{56.59}Fa_{43.41}$; 4, $Fo_{57.44}Fa_{42.56}$; 5, $En_{32.62}Fs_{24.40}Wo_{42.98}$; 6, $En_{32.59}Fs_{26.74}Wo_{40.66}$; 7, $En_{25.09}Fs_{65.94}Wo_{8.96}$; 8, $En_{25.79}Fs_{62.39}Wo_{10.81}$; 9, $En_{47.67}Fs_{49.25}Wo_{3.07}$; 10, $An_{47.93}Ab_{50.11}Ort_{1.95}$; 11, $An_{11.70}Ab_{86.55}Ort_{1.74}$; 12, $An_{81.40}Ab_{18.02}Ort_{0.58}$; 13, $An_{61.02}Ab_{37.24}Ort_{1.74}$; 14, $Ort_{93.31}Ab_{6.69}$. Aug, augite; Kfsp, K-feldspar; Ol, olivine; Opx, orthopyroxene; Pgt, pigeonite; Pl, plagioclase.
*According to SEM EDS; other analyses performed on a microprobe analyzer.
**Formulas based on number of oxygens.

formation, which accounts for their chemical similarity. Spurrite-merwinite marbles show large ranges in the ontents of CaO (50.72–53.67 wt.%), SiO_2 (7.62–21.18 wt.%), and Al_2O_3 (2.45–6.51 wt.%), as well as in LOI (12.23–32.28 wt.%), mainly at the account of CO_2. They have low Fe_2O_{3tot} (1.29–3.45 wt.%) and MgO (1.17–2.65 wt.%), within 0.2 wt.% MnO, Na_2O, K_2O and P_2O_5, and up to 2 wt.% SO_3. Wollastonite marbles bear up to 0.70 wt.% Na_2O. The ranges of major oxides are controlled by relative percentages of silicate and carbonate layers.

Mineral assemblages in marbles from the northern aureole part reveal five zones (Fig. 2*B*).

Zone 1. 1–3 cm: pyroxene-garnet skarn with calcite at the intrusion top (Pertsev, 1977).

Zone 2. ≥ 30 cm: spurrite-merwinite-monticellite-gehlenite marble (±rankinite, bredigite, cuspidine, (Zn,Fe)S), likewise within the top part of the intrusion (Fig. 4). Predominant minerals are calcite, spurrite (up to 50%) ($Ca_{4.8–5.0}Na_{0.0–0.1}Si_{1.8–2.0}P_{0.0–0.1}O_8(CO_3)$) and zoned melilite (within 20%) ($Gehl_{66–77}Ak_{16–24}Fe–Ak_{1–19}Na–Mel_{0–11}$ core; $Gehl_{41–71}Ak_{17–37}Fe–Ak_{0–25}Na–Mel_{2–10}$ rim) (Table 3). Merwinite ($Ca_{2.9–3.0}Na_{0.0–0.1}Mg_{0.8–1.0}Fe_{0.1–0.2}Si_{2.0}O_8$) varies from sporadic inclusions to 10 –17%. The total amount of monticellite ($Ca_{1.0}Mg_{0.6–0.8}Fe_{0.1–0.3}Mn_{0.0–0.1}Si_{1.0}O_4$) is <10%. It forms symplectites with spurrite or less often with cuspidine; isolated grains are rare. Calcite layers contain disseminated fine grains of melilite and merwinite. Perovskite is uniformly distributed over the rock while sulfides (pyrrhotite, rasvumite, djerfisherite, Fe-sphalerite and würtzite, and alabandine) are restricted to silicate layers and their boundaries.

Zone 3. Spurrite-melilite marble with perovskite, discovered as scattered blocks (Pertsev, 1977). It originally occurred about 1 m above the contact, judging by the description (Pertsev, 1977).

Zone 4. Tilleyite ($Ca_{4.8–5.0}Mg_{0.0–0.03}Na_{0.0–0.02}Si_{1.9–2.0}O_7(CO_3)_2$) marbles with wollastonite or parawollastonite and melilite (Fig. 4*E*) ($Gehl_{7–44}Ak_{28–68}Fe–Ak_{0.0–32}Na–Mel_{9–40}$) (± kalsilite, cuspidine, grossular), likewise discovered as scattered blocks up to 1 m; 1.5–2.7 m above the contact.

Zone 5. Marmorized limestones with partially recrystallized fauna and 1–3 mm pelitic layers replaced by fine aggregates of diopside and plagioclase (±amphibole, grossular); ≥ 3 m above the contact.

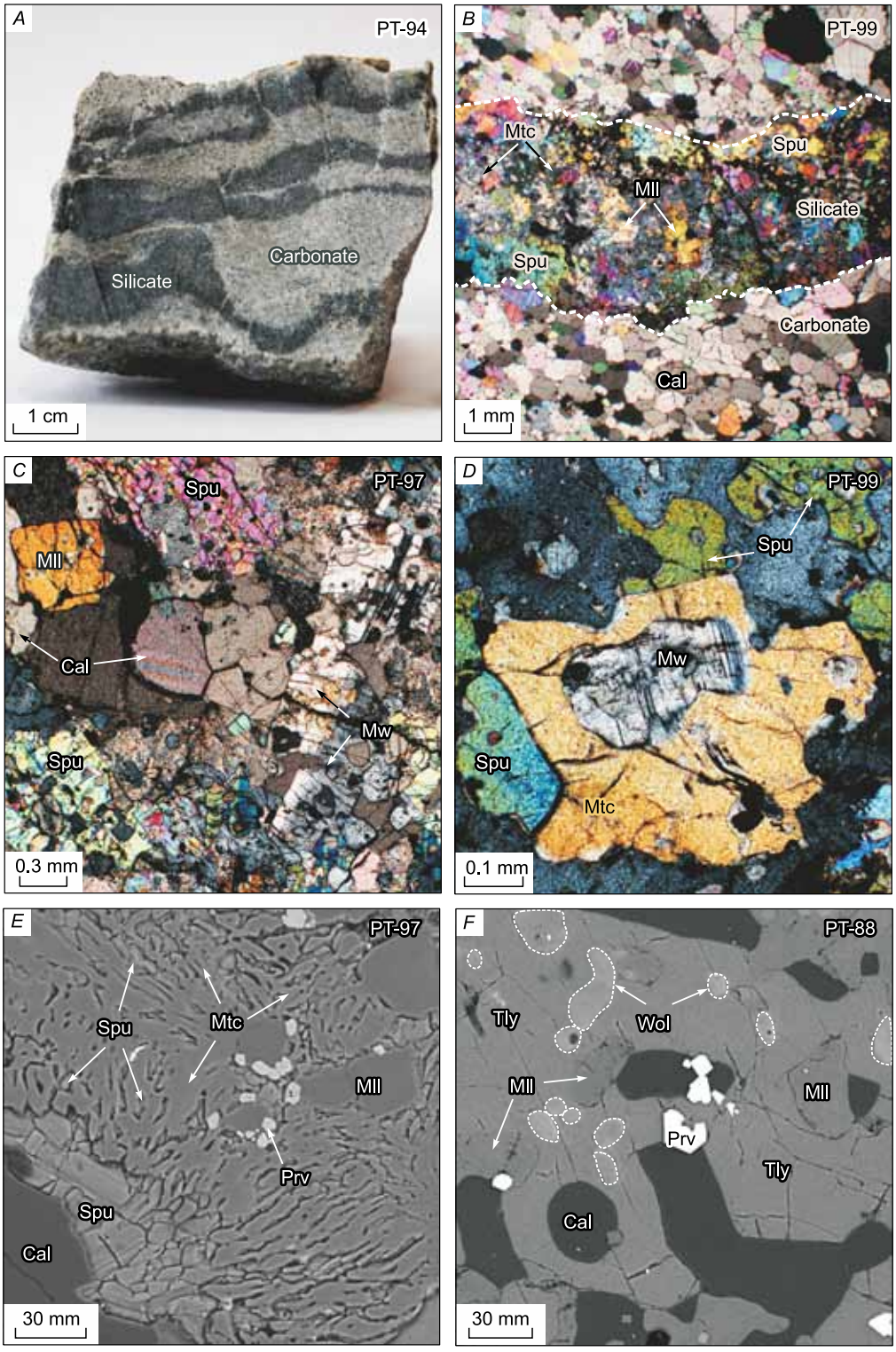

Fig. 4. Marbles from contact metamorphic site in the Kochumdek River valley. Typical spurrite-merwinite marble (*A*); silicate layer (*B*); calcite + spurrite + merwinite + melilite (*C*); relict merwinite inside monticellite (*D*); spurrite-monticellite symplectite (*E*); tilleyite with inclusions of calcite, wollastonite and perovskite (*F*). *A–D* are cross polarized light images; *E–F* are back-scattered electron images. Cal, calcite; Mll, melilite; Mtc, monticellite; Mw, merwinite; Prv, perovskite; Spu, spurrite; Tly, tilleyite; Wol, wollastonite.

Table 3. Representative analyses of rock-forming minerals from marbles in the Kochumdek contact aureole (wt.%)

Component	LLD	1*	2	3	4	5	6*	7	8	9	10*	11*	12	13
		Rnk	Brd	Mw		Mtc		Spu	Tly	Wol	Mll			
SiO_2	0.03	41.55	35.37	35.69	36.40	36.99	36.20	26.99	25.51	51.52	26.78	29.91	38.26	36.89
Al_2O_3	0.03	<0.30	bd.	bd	bd	bd	<0.30	bd	bd	bd	26.85	23.81	11.17	12.67
FeO	0.06	<0.30	0.96	3.65	2.04	5.63	11.49	bd.	bd	bd	1.89	1.49	4.04	5.94
MnO	0.06	<0.30	0.28	0.43	0.18	1.94	2.80	bd	bd	bd	<0.30	<0.30	0.27	0.24
MgO	0.04	<0.30	5.01	9.97	11.52	19.14	14.29	0.06	bd	0.10	2.75	4.13	6.24	5.72
CaO	0.03	58.58	57.39	49.67	48.85	36.23	35.61	61.78	58.13	48.53	39.60	39.40	37.46	37.96
Na_2O	0.06	<0.30	0.27	0.25	0.17	bd	<0.30	0.19	0.08	bd	0.31	0.62	1.84	1.62
K_2O	0.03	<0.30	0.11	bd	bd	bd	<0.30	bd	bd	bd	<0.30	<0.30	0.31	0.30
P_2O_5	0.02	<0.30	bd	0.13	0.05	bd	<0.30	0.13	bd	bd	<0.30	<0.30	bd	bd
Total	–	100.13	99.39	99.80	99.22	99.93	100.39	89.15	83.72	100.15	99.01	99.36	99.59	101.34
Formula based on	–	7 O**	16 O**	8 O**		4 O**		K 7		3 O**	7 O**			
Si	–	1.980	4.007	1.991	2.002	1.002	1.007	2.014	2.027	0.994	1.250	1.370	1.766	1.707
Al	–	0.000	0.000	0.000	0.000	0.000	0.000	0.000	0.000	0.000	1.480	1.290	0.608	0.691
Fe	–	0.000	0.091	0.170	0.107	0.127	0.267	0.000	0.000	0.000	0.070	0.060	0.150	0.160
Mn	–	0.000	0.027	0.020	0.011	0.044	0.066	0.000	0.000	0.000	0.000	0.000	0.010	0.009
Mg	–	0.000	0.846	0.828	0.891	0.772	0.592	0.006	0.000	0.003	0.190	0.280	0.429	0.394
Ca	–	2.991	6.967	2.969	2.971	1.052	1.061	4.940	4.948	1.004	1.980	1.940	1.853	1.882
Na	–	0.000	0.059	0.027	0.020	0.000	0.000	0.028	0.012	0.000	0.003	0.006	0.165	0.145
K	–	0.000	0.016	0.000	0.000	0.000	0.000	0.000	0.000	0.000	0.000	0.000	0.018	0.018
P	–	0.000	0.000	0.006	0.002	0.000	0.000	0.008	0.000	0.000	0.000	0.000	0.000	0.000

Note. TiO_2, BaO, SrO are below detection limit. LLD, detection limits of respective elements; bd, below detection limit. Analyses 3, 10, 12 are for core; analyses 4, 11, 13 are for rim; 5, Mtc–Spu symplectite; 6, isolated grain. For melilite: total iron as FeO; Fe = Fe^{3+} + Fe^{2+}. Mineral assemblages: 10, 11, Mw + Mtc +Mll + Spu + Cal ± Csp; 12, 13, Tly + Wol + Mll +Cal; 10, $Gehl_{70.5}Ak_{19.3}Fe–Ak_{7.5}Na\text{-}Mll_{2.8}$; 11, $Gehl_{0.6}Ak_{28.2}Fe–Ak_{6.7}Na–Mll_{5.5}$; 12, $Gehl_{20.7}Ak_{44.5}Fe–Ak_{16.7}Na–Mll_{17.9}$; 13, $Gehl_{25.7}Ak_{41.3}Fe–Ak_{17.1}Na–Mll_{15.9}$; for monticellite: 5, $Mtc_{81.8}Kirh_{13.5}Gla_{4.7}$; 6, $Mtc_{64.0}Kirh_{28.8}Gla_{7.1}$. Brd, bredigite ($Ca_7Mg[SiO_4]_4$); Cal, calcite; Gla, glaucochroite ($CaMn[SiO_4]$); Csp, cuspidine ($Ca_4Si_2O_7(F,OH)_2$); Kirh, kirschsteinite ($CaFe[SiO_4]$); Mll, melilite (Gehl, gehlenite ($Ca_2Al_2[SiO_7]$); Ak, akermanite ($Ca_2Mg[Si_2O_7]$); Fe–Ak, ferroakermanite ($Ca_2Fe[Si_2O_7]$); Na–Mll, Na–melilite ($CaNaAl[Si_2O_7]$); Mtc, monticellite ($CaMg[SiO_4]$); Mw, merwinite ($Ca_3Mg[SiO_4]_2$); Rnk, rankinite ($Ca_3[Si_2O_7]$); Spu, spurrite ($Ca_5[SiO_4]_2(CO_3)$); Tly, tilleyite ($Ca_5[Si_2O_7](CO_3)_2$); Wol, wollastonite.

*According to SEM EDS; other analyses performed on a microprobe analyzer.

**Formulas based on number of oxygens; K7 means formula based on cations.

Parameters of metamorphism. Temperature reconstructions for contact metamorphism require the knowledge of silicate-carbonate equilibrium temperatures which depend largely on P_{tot} and P_{CO_2} (Reverdatto, 1970; Pertsev, 1977; Tracy and Frost, 1991; Grapes, 2011). According to the total thickness of sediments over the intrusion (~665-m), overburdern pressure at the onset of metamorphism was ~ 200 bar, which agrees with early estimates (Reverdatto, 1964); the CO_2 pressure was $P_{CO_2} \le 0.2\ P_{tot}$ (Pertsev, 1977).

The range of temperatures that induced retrograde metamorphism of the Kochumdek marbles was reconstructed with reference to phase transformations involving merwinite which were plotted theoretically or empirically for some compositions in the gehlenite–akermanite series (Pertsev, 1977; Tracy and Frost, 1991; Grapes, 2011). This temperature range is constrained by the merwinite + calcite → spurrite + monticellite (T_{min} = 820 °C for $P_{CO_2} = 0.2\ P_{tot}$) reaction from below and by the stability of the merwinite + melilite assemblage ($Gehl_{80}$) (T_{min} = 880 °C for $P_{CO_2} = 0.2\ P_{tot}$) from above (Pertsev, 1977). The presence of rankinite, bredigite, and a (Zn, Fe, Mn)S high-temperature modification (type of würtzite) indicate $T \ge 900$ °C temperatures at the contact. The polymorphic transition $(Zn,Fe)S_{hex} \rightarrow (Zn,Fe)S_{cub}$, which is possible at T = 894 °C (P = 150 bar), provides a mineral thermometer independent of P_{CO_2} (Kullerud, 1953). Thus, the protolith in the merwinite zone should be heated to $T \ge 900$ °C. In its turn, the akermanite + calcite → merwinite equilibrium allows estimating the fraction of $P_{CO_2} \sim 0.5P_{tot}$ at known P_{tot} = 200 bar and $T \ge 900$ °C (Tracy and Frost, 1991; Grapes, 2011). The presence of the pyrrhotite + rasvumite assemblage and the absence of pyrite in all analyzed marble samples, along with experimental data for the system $KFeS_2$–Fe–S (Osadchii et al., 2018), place the lower constraint on the temperature of metamorphism in zones 2–4 at 513 °C.

In general, the set of minerals, such as rankinite, bredigite, spurrite, melilite ($Gehl_{66–77}$) (zone 2); spurrite (zone 3); tilleyite, wollastonite, and melilite ($Gehl_{<45}$) (zone 4); diopside, amphibole, grossular (zone 5), indicate the following

minimum temperatures of sediments over the Kochumdek intrusion (Fig. 2): ≥ 900 °C for zone 2; ≥ 750 °C for zone 3; ≥ 700 °C for zone 4; and ~ 500–550 °C for zone 5 (Reverdatto, 1970; Pertsev, 1977; Tracy and Frost, 1991; Heinrich et al., 2004; Grapes, 2011). These values were used for reference in the formulation and solution of thermophysical problems.

PROBLEM FORMULATION

The heat transfer problem was solved for real parameters of metamorphic zonation around a sill in the Kochumdek valley. Modeling is performed in a 2000 m long and 1120 or 1200 m high domain with three subdomains corresponding to geological bodies (trap intrusion and country rocks above and below); the vertical size of the model domain varies according to the assumed intrusion thickness. The upper and lower subdomains corresponding to sediments are, respectively, 700 and 440 m thick heat conducting solids. The central subdomain is a horizontal conduit filled with flowing or stagnant melt, varying in thickness from 20 to 100 m in different model versions (Fig. 5). The model grid consists of 2000 points spaced at 1 m along the x axis and 0.5 m along the y axis; the grid spacing reduces near the contacts along the y axis (up to 0.05 m in the sedimentary layers) in all three subdomains. The assumed initial temperatures are T_0 = 30 °C in sediments and 1120 to 1200 °C in magma at the conduit input. The boundary condition is isothermal (30 °C) on the domain top and adiabatic along other boundaries. Pressure exceeds the overburden value (ΔP) at the conduit input but equals this value (0.2 kbar = 20 MPa) at the output.

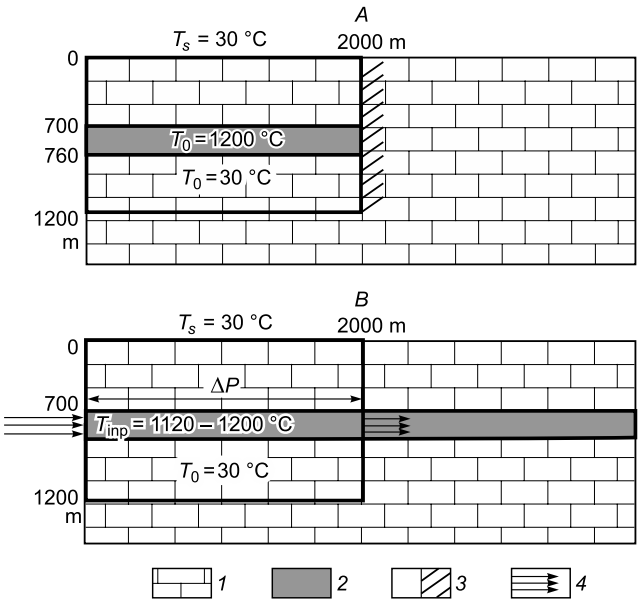

Fig. 5. Two models of thermal regime during emplacement of the Kochumdek intrusion. *A*: Model 1. Magma fills up the conduit "instantly", does not flow and cools down conductively. *B*: Model 2. Prolonged magma flow in the conduit is driven by pressure gradient, with regard to crystallization dynamics and temperature dependence of magma viscosity. Symbols are explained in text. *1*, sediments; *2*, conduit with magma; *3*, tight wall; *4*, flow direction.

Fluid dynamics in the magma conduit is described by complete Navier-Stokes equations with regard to crystallization enthalpy, variable viscosity, and melt density. The formalism was detailed previously (Semenov and Polyansky, 2017). The problem is solved using the *ANSYS Fluent* (2009) software. Within the solidus-liquidus temperature range, magma is simulated as a porous material with porosity equal to melt fraction and a single-phase liquid with averaged flow rate for a discrete material volume containing a mixture of crystalline and liquid components. The crystallization heat is linearly proportional to percentage of the crystalline phase.

The density and crystallinity of magma flowing along the conduit, as well as the solidus and liquidus temperatures, were calculated using the *MELTS* software (Ghiorso and Sack, 1995) for real compositions of troctolite dolerite and gabbro-dolerite from the contact aureole (Table 1). Magma viscosity, as estimated with reference to an empirical relationship taking into account bulk chemistry of mafic rocks and water content in the melt (Persikov and Bukhtiyarov, 2009), changed from 60 to 5×10^6 Pa s upon cooling from 1250 to 1050 °C. In all studied dolerite compositions, ~1000 °C magma contained 98–99% of crystals. Heat capacity, thermal conductivity, and density of the host sediments were, respectively, 860 J/kg K, 2.4 W/m K, 2650 kg/m^3; the respective values for magma were 1250 J/kg K, 2.5 W/m K, and 2660–3060 kg/m^3; the crystallization enthalpy of magma was assumed to be 380 kJ/kg according to (Gutierrez and Parada, 2010). The initial melt contained 0.5 wt.% of water.

NUMERICAL RESULTS

The simulation aimed at constraining the heat source regime to provide satisfactory explanation for the temperature distribution in the Kochumdek aureole of contact metamorphism (Fig. 2). The solutions were checked against geothermometer-based temperature estimates. The temperature distribution near the heat source (magma conduit) was considered as having successively several controls (1) magma flow; (2) conduit thickness; (3) initial magma temperature; (4) crystallization enthalpy; (5) thermal conductivity and heat capacity of sediments.

Model 1. Conductive cooling of basaltic magma with its initial temperature of 1200 °C, which "instantly" fills up a 60 m thick conduit and does not flow afterwards (Fig. 5*A*). The temperature at the contact for this case (cooling and heat release upon crystallization of a stagnant melt) does not exceed 790 °C and decreases with time (Fig. 6). Note that neither a thicker conduit (100 m instead of 40 m) nor better heat conducting properties of sediments can increase this

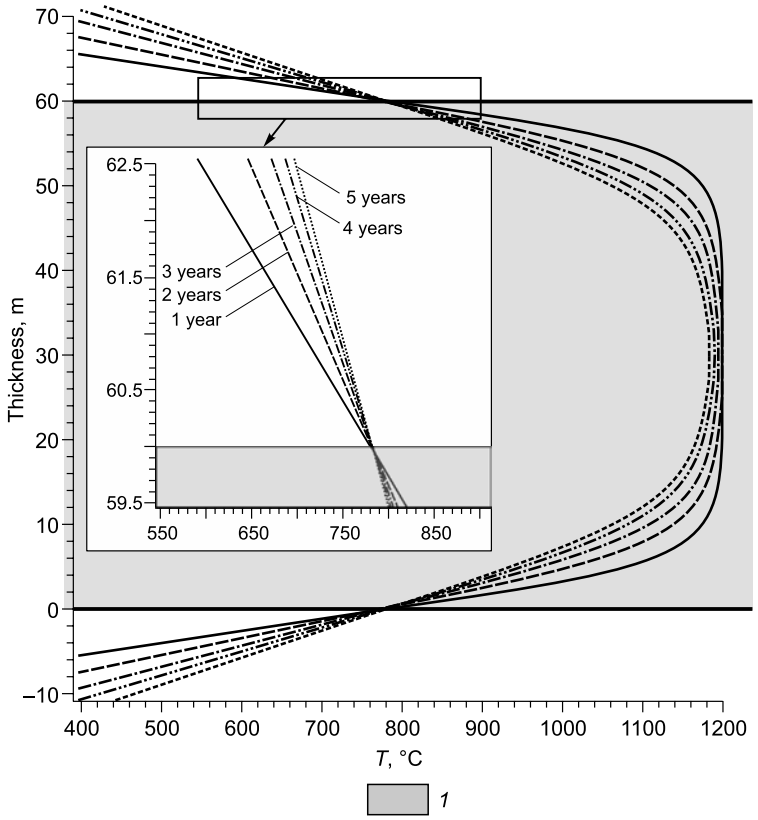

Fig. 6. Calculations for model of magma crystallization (*A* in Fig. 5) with T_0 = 1200 °C in a 60 m thick conduit. Temperature profiles are shown for time periods of 1 to 5 years. *1*, sill.

temperature in the absence of magma flow. The model predicts only that thermal metamorphism gradually expands and reaches a thickness of 5 m in 5 years (Table 4). Thus, cooling of a stagnant melt fails to account for the ≥ 900 °C temperature along the intrusion margins inferred from the mineralogy.

Additional calculations were applied to estimate the contribution of crystallization enthalpy for basaltic magma to the heat budget of the system. It was found out to be responsible for ~100 °C temperature increase (the temperature at the contact would be ≤ 680 °C without it), which is insufficient to provide the required temperatures at control points anyway.

Model 2. A more complex case of magma flow in the conduit and convective heat transfer (Fig. 5*B*); pressure at the conduit input exceeding the overburden pressure (P_{ovbd} = 20 MPa), with Δ*P* from 0.001 MPa to 10 MPa; magma temperature at the conduit input from 1120 to 1200 °C in different model versions. The pressure gradient holds for 30 days and drives magma flow, which then stops and the stagnant magma cools down. The temperatures near the intrusion-sediment contact calculated at T_0 = 1200 °C and Δ*P* = 1 MPa (5% of the overburden) are as shown in Fig. 7. Model 2 yields higher temperatures of the sediments (*T* ≥ 800 °C) than Model 1, and the width of the hot zone corresponds to the intersection of temperature curves at 0.6-0.8 m above the contact (see inset in Fig. 7). The sediments remain hot for 35 or 5 years at conduit thicknesses of 60 m and 20 m, respectively.

If magma does not flow and cools down conductively (Model 1), the temperature curves intersect at the conduit boundary (Fig. 6), which rules out the existence of a contact aureole around the conduit. Meanwhile, magma flow for one month (convective heat transfer, Model 2) is sufficient to heat up the adjacent sediments to *T* = 900 °C; after that time, the flow stops and magma cools down by conduction. The profile of maximum temperatures for six months of cooling fits the best the temperature distribution at control points of the Kochumdek metamorphic complex (Fig. 7).

Models with conduit thicknesses from 40 to 100 m and magma flow durations exceeding one year yield temperatures at least 100 °C hotter than those inferred from indicator minerals at control points and thus contradict the observations. The temperatures are as high as that also at longer magma flow duration (at least two years) in a thinner conduit (20 m), at a pressure excess of ≥0.1 MPa. Rapid magma flow entrains crystals, and no continuous solidification can occur near the conduit walls. Unlike Model 1, the temperature of flowing magma in Model 2 does not decrease much near the contact with sediments, while the conduit remains a stationary heat source.

Additionally, heat loss was estimated in terms of Model 2 as a function of the thermal properties of wallrock car-

Table 4. Evolution of temperature field near a trap intrusion in the middle of modeling domain for 5 years at different distances from the contact (°C)

Thickness, m	1 year				5 years			
	Distance from contact, m							
	Contact	5 m	25 m	50 m	Contact	5 m	25 m	50 m
20	770	400	30	30	750	545	30	30
40	778	410	30	30	785	560	30	30
60	780	410	30	30	785	580	32	30
80	780	415	30	30	790	585	34	30
100	785	420	31	30	790	585	34	31

Note. Initial magma temperature at conduit input: 1200 °C.

bonate sediments: 700 to 1100 J/kg K heat capacity and 0.8 to 3 W/m K thermal conductivity. The calculations allowed for the contribution of exothermic phase change by decreasing the effective heat capacity of sedimentary rocks. The results show that heat loss from magma flowing along a conduit pays the greatest contribution into the total heat budget. Endothermic phase change in carbonate sediments consumes almost as much heat as that released by crystallization (Dudarev et al., 1972), and the two components cancel each other. As the model magma temperature at the conduit (T_{in}) input decreases from 1200 to 1150°C, the temperatures at control points require magma flow durations of 6–8 months instead of one month.

DISCUSSION

Marbles formed in two zones along intrusion margins (Kuzmovka sill in the right side of the Podkamennaya Tunguska River and an intrusion in the Kochumdek middle reaches) by the same mechanism from the same sedimentary protolith, at an overburden pressure of ~200 bar. According to data on mineral assemblages, the temperatures at the top of the two intrusions were $T \sim 740$ °C for the 150-m thick Kuzmovka sill (Reverdatto, 1964, 1970; Pertsev, 1977) and >900 °C for the ≤80 m Kochumdek intrusion. Therefore, thermal metamorphism in the latter case differed from that common to the southwestern Tunguska basin, apparently

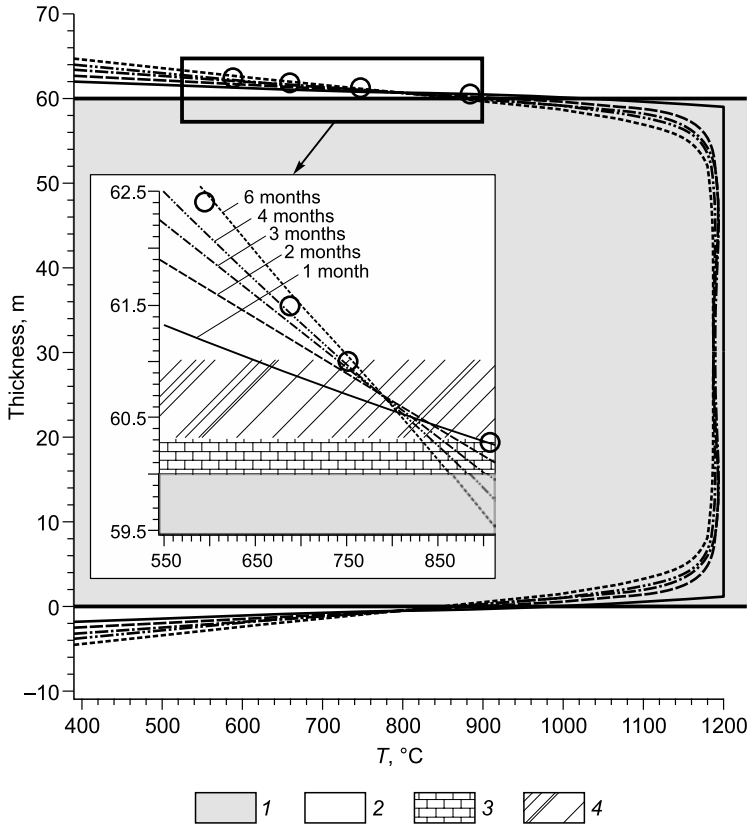

Fig. 7. Calculations for model of magma flow (*B* in Fig. 5) with T_0 = 1200 °C in a 60 m thick conduit under a pressure gradient of 1 MPa. Temperature profiles are shown for a time period of 1 to 6 months. Inset enlarges a contact fragment at the upper intrusion margin. Circles are temperatures at different distances from the contact estimated from mineral thermometers. *1*, sill; *2*, country rock; *3*, spurrite-merwinite marbles; *4*, spurrite marbles.

due to emplacement features of the Kochumdek complex. Good fit of the computed temperature distribution in the presence of magma flow to field data allows us to interpret the Kochumdek marbles as carbonate sediments metamorphosed by heating from flowing basaltic magma. In this respect, the complex is similar to a dolerite sill from the Isle of Mull in Scotland (Wartho et al., 2001), with the only difference that the latter emplaced into pelitic sediments. The models we obtained allow first estimates for the duration of different stages in the metamorphic process with reference to the results reported for the Mull Isle sill (Wartho et al., 2001).

The available models explaining thermal regime around sills and dikes are of two main types: precritical or postcritical operation of the magma-wall rock system (Sharapov et al., 2000). In the precritical case, the pressure gradient is too low to maintain magma flow in the conduit, and the chamber becomes "instantly" filled up with magma which cools down conductively and solidifies. The pressure gradient at the postcritical regime is sufficient for stationary magma flow, and high heat transfer from magma to the wallrock provides high temperature in the aureole while the flow holds.

Thermal effects on the extent, duration, and maximum temperature of contact metamorphism in the absence of fluids were a subject of many studies (Dudarev et al., 1972; Sharapov et al., 2000; Nabalek et al., 2012; Reverdatto et al., 2019). According to Dudarev et al. (1972), the maximum temperatures at the contact calculated for a conductive model "stagnant magma – wall rock" do not exceed 650–700 °C; the aureole in carbonate sediments around a 20 to 100 m thick sill (dike) is 0.5–2.5 m wide; heating of rocks to T = 500 °C takes from 1.7 to 26 years. Convection of pore fluids in the sediments and heat released upon crystallization cause a minor effect on the duration of sill cooling (Polyansky et al., 2002, 2003), and can be neglected.

The effect from the Mull Isle sill was different (Wartho et al., 2001): the temperature at the contact reached 930 °C; the host schists along the sill margin were molten and recrystallized. Wartho et al. (2001) inferred the existence of a turbulent magma flow of T = 1130 °C along a 6 m thick conduit for five months, from reactions observed in minerals and loss of radiogenic argon (^{40}Ar) from micas. The excess pressure reached 29 MPa, while the overburden pressure was 250 MPa (corresponding to a depth of 8.3 km).

As shown by our calculations, the temperature profile of the Kochumdek zone of contact metamorphism could result from a stationary magma flow in a conduit at T = 1120–1200 °C existing for a few months, at a pressure excess of ~1 MPa. Thus, the estimated magma flow lifetime required for the formation of spurrite-merwinite marbles around the Kochumdek intrusion is similar to that for the Mull sill (Wartho et al., 2001), but the excess pressure we obtained is much lower: 1 MPa against 29 MPa. This difference is reasonable given that the two magma chambers occur at different depths (0.7 km and 8.3 km, respectively). Our modeling showed that the intrusion thickness does not affect the maximum temperature of contact metamorphism but controls the duration of wall rock heating and the thickness of low-temperature zones of metamorphism.

The distribution of flow rates across the conduit corresponds to the Poiseuille parabolic profile with the maximum (1.2 m/s at ΔP = 1 MPa) at the conduit axis. The amount of magma flowing through a 60 m thick and 1 km long conduit for three months, estimated assuming an average flow rate of 0.8 m/s along the whole profile, is ~350 km^3. It is, however, hard to estimate the total volume of the Kuzmovka igneous rocks for the lack of drilling data; the amount of emplaced magma can be approximately inferred from the surface area occupied by basaltic rocks. The volume of magma released through a 1 km long conduit corresponds to a 100 m thick intrusion over an area of 50 × 70 km, which appears to be quite realistic (Fig. 1).

CONCLUSIONS

The Kochumdek zoned metamorphic complex is located at the contact between the upper margin of a differentiated trap intrusion (troctolite gabbro-dolerite, Kuzmovka complex) and marly limestones of the lower Kochumdek subformation. The overburden pressure at the time of emplacement was about 200 bar. The diversity of indicator minerals allows reconstructing temperature ranges for four metamorphic zones in the aureolse: $T \geq$ 900 °C for zone 2 (merwinite, spurrite, gehlenite (± rankinite, bredigite)); $T \geq$ 750 °C for zone 3 (spurrite); $T \geq$ 700 °C for zone 4 (tilleyite and melilite ($Gehl_{<50}$)); and T = 500–550 °C for zone 5 (diopside, amphibole, and grossular). Retrograde decomposition of merwinite producing spurrite-monticellite or cuspidine-monticellite symplectites indicates that the temperature of retrograte metamorphism in zone 2 was maintained at 820–880 °C. The metamorphic zones gradually become thicker from >30 cm near the contact to >1 m away from it.

Numerical methods were applied to analyze various controls of temperatures in the contact aureole: magma flow along the conduit, magma temperature, conduit thickness, and thermal properties of host sediments. The sought temperatures at the control points in the aureole can be achieved in the presence of magma flow for a few months.

The computed temperature profiles for the Kochumdek complex agree well with those inferred from mineral thermometers at the following parameters: magma temperature 1200 °C; intrusion thickness >40 m; magma flow duration up to a few months. The respective temperatures require a more prolonged magma flow of one year through a ≤20 m thick conduit. This lifetime is inversely proportional to the initial temperature of magma. Yet, crystallization of a stagnant melt fails to cause spurrite-merwinite metamorphism ($T \geq$ 800 °C). The modeling also provides constraints on the aureole thickness where two zones of maximum temperatures are located: 0.6–0.8 m (inset in Fig. 7). These zones can develop for 5 to 35 years if the intrusion is from 20 to 60 m thick.

Thus, the model simulating the formation of the Kochumdek marbles has confirmed the earlier inference (Reverdatto, 1970) that nothing but magma flow through a conduit can heat up sediments (mainly dry) along the intrusion margin to temperatures ~ 850–900 °C, or above those at conductive heat transfer. The exact conduit geometry (dike vs. low-angle sill) remains unclear because of poor exposure. According to Reverdatto (1970), magma flow along a fracture in the case of a dike provides satisfactory explanation for the estimates of temperature distribution and their evolution in the contact aureole we obtained by modeling. Furthermore, metamorphism around a sill appears unlikely because pressure-driven magma flow was restricted to a short spell when the magma chamber was filled up, while composition differentiation in thick sills of the Kuzmovka complex indicates that the convective component was minor.

We wish to thank P.V. Kochkarev, director of the Central Siberian biospheric reserve and the reserve team, as well as A.P. Gustomesov, head of the Kochumdek Factoria, for assistance in field work. Thanks are extended to Professor A.E. Izokh from IGM for useful advice and to N.S. Karmanov, E.N. Nigmatulina and M.V. Khlestov from the Analytical Center of the V.S. Sobolev Institute of Geology and Mineralogy (Novosibirsk) for analytical work. We specially appreciate interest to our study and support by E.V. Sklyarov, chief editor of Russian Geology and Geophysics. The manuscript profited from constructive criticism by I.I. Likhanov and A.V. Lavrenchuk, the reviewers.

The study was supported by grants 15-05-00760 and 17-05-00848 from the Russian Foundation for Basic Research and was carried out as part of a government assignment to IGM.

REFERENCES

Alekseenko, V.D., Alasev, V.A., Barmin, V.A., Belolipetskaya, L.I., Bozhko, V.V., Varganov, A.S., Egorov, V.N., Egorov, A.S., Kazhaeva, O.D., Kachevsky, L.K., Moskalev, V.A., Pevzner, V.S., Radyukevich, N.M., Rumyantsev, N.N., Suslova, S.V., Shor, G.M., 2010. State Geological Map of the Russian Federation, Scale 1:1 000 000 (third generation). Ser. Angara-Yenisei. Sheet R-46-North Yenisei. Explanatory Note [in Russian]. Kart. Fabrika VSEGEI, St. Petersburg.

ANSYS Fluent Theory Guide, 2009. Release 12.1.

Dudarev, A.N., Kudryavtsev, V.A., Melamed, V.G., Sharapov, V.N., 1972. Heat Transfer in Magma Generation Processes [in Russian]. Nauka, Novosibirsk.

Egorova, V., Latypov, R., 2013. Mafic-ultramafic sills: New insights from M- and S-shaped mineral and whole-rock compositional profiles. J. Petrol. 54 (10), 2155–2191.

Galuskin, E.V., Kusz, J., Armbruster, T., Bailau, R., Galuskina, I.O., Ternes, B., Murashko, M., 2012. A reinvestigation of mayenite from the type locality, the Ettringer Bellerberg volcano near Mayen, Eifel district, Germany. Mineral. Mag. 76 (3), 707–716.

Galuskina, I.O., Galuskin, E.V., Armbruster, T., Lazic, B., Dzierzanowski, P., Gazeev, V.M., Prusik, K., Pertsev, N.N., Winiarski, A., Zadov, A.E., Wrzalik, R., Gurbanov, A.G., 2010. Bitikleite-(SnAl) and bitikleite-(ZrFe): New garnets from xenoliths of the Upper Chegem volcanic structure, Kabardino-Balkaria, Northern Caucasus, Russia. Am. Mineral. 95, 959–967.

Gazeev, V.M., Gurbanova, O.A., Zadov, E.A., Gurbanov, A.G., Leksin, A.B., 2012. Mineralogy of skarn limy xenoliths of Shadil-hoh volcano (Kel volcanic area of the Great Caucasus). Vestnik Vladikavkazskogo Nauchnogo Tsentra, No. 2, 23–33.

Ghiorso, M.S., Sack, R.O., 1995. Chemical mass transfer in magmatic processes IV. A revised and internally consistent thermodynamic model for the interpolation and extrapolation of liquid-solid equilibria in magmatic systems at elevated-temperatures and pressures. Contrib. Mineral. Petrol. 119 (2–3), 197–212.

Grapes, R., 2011. Pyrometamorphism (second edition). Springer, Berlin.

Gutierrez, F., Parada, M.A., 2010. Numerical modeling of time-dependent fluid dynamics and differentiation of a shallow basaltic magma chamber. J. Petrol. 51 (3), 731–762.

Heinrich, W., Churakov, S.S., Gottschalk, M., 2004. Mineral-fluid equilibria in the system $CaO–MgO–SiO_2–H_2O–CO_2–NaCl$ and the record of reactive fluid flow in contact metamorphic aureoles. Contrib. Mineral. Petrol. 148, 131–149.

Kerrick, D.M. (Ed.), 1991. Contact Metamorphism. Ser. Rev. Mineral. Mineral. Soc. Am. Washington, D.C.

Khoury, H., Sokol, E., Kokh, S., Seryotkin, Y., Kozmenko, O., Goryainov, S., Clark, I., 2016. Intermediate members of the lime-monteponite solid solutions ($Ca_{1–x}Cd_xO$, x = 0.36–0.55): Discovery in natural occurrence. Am. Mineral. 101, 132–147.

Koritnig, S., 1978. Die „Blaue Kuppe“ bei Eschwege. Aufschlug 28, 237–247.

Kullerud, G., 1953. The FeS–ZnS system: a geological thermometer. Norsk Geologisk Tidsskrift 32, 61–147.

Lebedev, A.P., 1962. Trappean magmatism in the lower Podkamennaya Tunguska, in: Petrography of East Siberia [in Russian]. Izd. AN SSSR, Moscow, Book 1, pp. 71–117.

Lungershausen, G.F., Schulz, N.E., Bogdanova, N.N., Dekhterev, G.B., 1959. Geological Map of the USSR, Scale 1: 200 000. Ser. Turukhansk, Sheet R-46-XIV [in Russian]. Gosgeoltekhizdat, Moscow.

Malich, N.S., Grigoriev, V.V., 1960. Correlation of magmatism and tectonics in the lower Podkamennaya Tunguska and Bakhta river basins, in: Geology and Mineral Resources in the Siberian Craton (VSEGEI Transactions, New Series, Issue 31) [in Russian]. VSEGEI, Leningrad pp. 27–36.

Nabelek, P.I., Hofmeister, A.M., Whittington, A.G., 2012. The influence of temperature-dependent thermal diffusivity on the conductive cooling rates of plutons and temperature-time paths in contact aureoles. Earth Planet. Sci. Lett. 317–318, 157–164.

Osadchii, V.O., Voronin, M.V., Baranov, A.V., 2018. Phase equilibria in the $KFeS_2–Fe–S$ system at 300–600 °C and bartonite stability. Contrib. Mineral. Petrol. 173, 44.

Persikov, E.S., Bukhtiyarov, P.G., 2009. Interrelated structural chemical model to predict and calculate viscosity of magmatic melts and water diffusion in a wide range of compositions and T–P parameters of the Earth's crust and upper mantle. Russian Geology and Geophysics (Geologiya i Geofizika) 50 (12), 1079–1090 (1393–1408).

Pertsev, N.N., 1977. High-Temperature Metamorphism and Metasomatism of Carbonate Rocks [in Russian]. Nauka, Moscow.

Pertsev, N.N., Shmulovich, K.I., 1972. Physicochemical conditions of larnite-merwinite facies contact metamorphism: a case study from the Podkamennaya Tunguska basin. Izvestiya AN SSSR, Ser. Geol., No. 6, 39–47.

Polyansky, O.P., Reverdatto, V.V., Sverdlova, V.G., 2002. Convection of two-phase fluid in a layered porous medium driven by the heat of magmatic dikes and sills. Geochem. Int. 40 (Suppl. 1), S69–S81.

Polyansky, O.P., Reverdatto, V.V., Khomenko, A.V., Kuznetsova, E.N., 2003. Modeling of fluid flow and heat transfer induced by basaltic near-surface magmatism in the Lena–Tunguska petroleum basin (Eastern Siberia, Russia). J. Geochem. Explor. 78–79, 687–692.

Poryadin, V.S., Strunin, B.M., Turchin, A.V., Komarov, V.V., Fainer, Yu.B., 1977. State Geological Map of the USSR, Scale 1: 200 000, Ser. Turukhansk, Sheet R-46-XIV. Explanatory Note [in

Russian]. Krasnoyarskoe Territorial'noe Geologicheskoe Upravlenie, Moscow.

Prusskaya, S.N., 2008. Petrology of Intrusive Trappean Magmatism in the Western Siberian Craton: Evidence from Petroleum Drilling [in Russian]. Siberian Federal University, Krasnoyarsk.

Reverdatto, V.V., 1964. High-temperature contact metamorphism of limestones in the Podkamennaya Tunguska basin. DAN SSSR 155 (1), 104–107.

Reverdatto, V.V., 1970. Facies of Contact Metamorphism [in Russian]. Nedra, Moscow.

Reverdatto, V.V., Likhanov, I.I., Polyansky, O.P., Sheplev, V.S., Kolobov, V.Yu. (Eds.), 2017. The Nature and Models of Metamorphism. Springer Geology, Switzcrland, Cham.

Semenov, A.N., Polyansky, O.P., 2017. Numerical modeling of the mechanisms of magma mingling and mixing: A case study of the formation of complex intrusions. Russian Geology and Geophysics (Geologiya i Geofizika) 58 (11), 1317–1332 (1665–1683).

Sharapov, V.N., Akimtsev, V.A., Dorovsky, V.N., Perepechko, Yu.V., Cherepanov, A.N., 2000. Dynamics of Ore-Magmatic Systems in Spreading Zones [in Russian]. Izd. SO RAN, Novosibirsk.

Sokol, E.V., Kokh, S.N., Khoury, H.N., Seryotkin, Yu.V., Goryainov, S.V., 2016. Long-term immobilization of Cd^{2+} at the Tulul Al Hammam natural analogue site, central Jordan. Appl. Geochem. 70, 43–60.

Tesakov, Yu.I., 2014. Validity of Silurian formations in the northwestern Siberian craton, from production geophysics. Novosti Paleontologii i Stratigrafii, Issue 19. Supplement to Russian Geology and Geophysics (Geologiya i Geofizika) 55, 5–37.

Tracy, R.J., Frost, B.R., 1991. Phase equilibria and thermobarometry of calcareous, ultramafic and mafic rocks, and iron formations, in: Kerrick, D.M. (Ed.), Contact Metamorphism. Rev. Mineral., Vol. 26. Mineral. Soc. Am., pp. 207–280.

Van Bergen, M.J., Barton, M., 1984. Complex interaction of aluminous metasedimentary xenoliths and siliceous magma: an example from Mt. Amiata (Central Italy). Contrib. Mineral. Petrol. 86, 374–385.

Wartho, J.-A., Kelley, S.P., Blake, S., 2001. Magma flow regimes in sills deduced from Ar isotope systematics of host rocks. J. Geophys. Res. Solid Earth 106 (B3), 4017–4035.

Editorial responsibility: E.V. Sklyarov